Atmospheric Neutral Density Experiment Risk Reduction (ANDE-RR) Flight Hardware Details

Andrew C. Nicholas, *
Ted Finne, †
Mark A. Davis, ‡

January 26, 2007

Overview

The ILRS community has requested particular documentation for all missions that the laser stations supports. The main purpose of this document is to be the repository of the raw measurements supporting this request for the ANDERR mission (Figure 1). These encompasses both the technical requirements for the laser based tracking and the target corrections to full exploit the data accuracy, precision, signature to further the science benefit of the field measurements. Using the example document from Appleby for the GIOVA mission as a template the following sections are provided to answer the 16 required questions that were formed in 2006 by the missions working group. Additionally, the inclusion and annotation of design, measured, and derived data has been attempted, so that collaborative assessment of performance will be possible. Further details can be found in the referenced documents, however if information is gathered outside this work, the authors request that it be requested to appear in updates to this document so as to further the template work by example of information needed to support the full ANDE and other ILRS supported missions.

Summary of LRA information and ILRS MWG questions

```
QUESTION 1) Array type (spherical, hexagonal, planar,etc.), to include a diagram or photograph.
ANSWER   1) Arrays are 19.0 inch and 17.5 inch diameter spherical objects with photos shown in
            Figure 2, 4 and 5.   Each spacecraft is fitted with a set of thirty 12.7 mm diameter
            optical retro reflectors for SLR located along latitudianl bands at + / - 90 deg,
            + / - 52.5 deg, and + / - 15 deg with one, six and eight retroreflectors per
            band respectively.

QUESTION 2) Array manufacturer.
ANSWER   2) Array is an US Naval Research Laboratory custom design by the Naval Center for Space
            Technology and with Implementation and fabrication by the NRL Space Sciences Division.

QUESTION 3) Link (URL or reference) to any ground-tests that were carried out on the array.
ANSWER   3) Ground testing on the array was not performed but the array is very similar that
            of Starshine3.  Surface measurement details in the references.
```

*Naval Research Laboratory, Code 7607, Thermospheric and Ionospheric Research and Applications Group, Washington D.C. 20375
†Naval Research Laboratory, Code 7607, Praxis Inc, Alexandria, VA 22303
‡Naval Research Laboratory, Code 8123, Electro-Optics Technology Sections, Honeywell Technology Solutions, Inc., Washington D.C. 20375

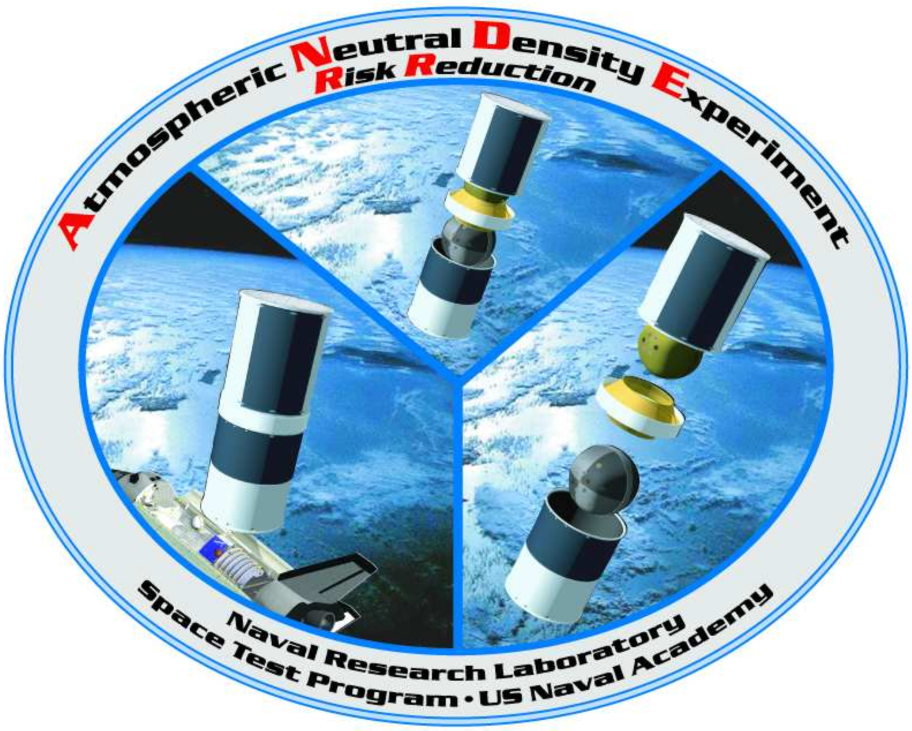

Figure 1: The ANDE Risk Reduction LOGO

QUESTION 4) The LRA design and/or type of cubes was previously used on the following mission:
ANSWER 4) The LRA design and type of cubes is similar to that used on the Starshine 1 and 3 Missions. See reference [Kessel], Figure 16 and details following. Analytically derived mean cross section is from 0.1 e6 + / - 0.05 e6 meters^2

QUESTION 5) The 3-D location (possibly time-dependant) of the satellite's mass centre relative to a satellite-based origin.
ANSWER 5) The 3D location of the center of mass is shown in Tables 1 and 2 and is bounded by 1.1 millimeter

QUESTION 6) The 3-D location of thte phase centre of the LRA relative to a satellite-based origin.
ANSWER 6) The optical phase center to satellite origin is 224.7 mm for the MAA (Active) and 205.2 mm for the FCAL (Passive). Relationship to origin will require attitude.

QUESTION 7) The position and orientation of the LRA reference point (LRA mass-centre or marker on LRA assembly) relative to a satellite-based origin.
ANSWER 7) The position of the LRA reference to the satellite origin is not needed for a sphere The mass properties have been included for long term spin vector determination.

QUESTION 8) The position (xyz) of either the vertex or the centre of the front face of each corner cube within the LRA assembly, with respect to the LRA reference point and including information of amount of recession of the front faces of cubes.
ANSWER 8) The vertex of each reflector is shown in Tables 1 and 2.
The recession is shown in Figure 12 and 15. The diameter of the hole exposing the aperture is 10.67 millimeters centered about the vertex aperture axis.

QUESTION 9) The orientation of each cube within the LRA assembly (three angles for each cube).
ANSWER 9) The orientation for each cube is radially outward. These are constructed so that the aperture is normal to the tangent of the sphere at each location. The tolerance is XXXX degrees.

QUESTION 10) The shape and size of each corner cube, especially the height.
ANSWER 10) The size and shape of each corner cube is shown in Figure 6 is Edmund NT45-202.
The height of these 10.2 mm COTS retro reflectors is measured to be 10.16 mm with + or - 0.25 mm uncertainty.

QUESTION 11) The material from which the cubes are manufactured (e.g. quaratz);
ANSWER 11) The Material for each corner cube is BK7.

QUESTION 12) The refractive index of the cube material, at a range of wavelengths.
ANSWER 12) The refractive index of the cube material BK7 is 1.53815 for 355 nm, 1.52805 for 423.5 nm 1.51947 for 532 nm, 1.50991 for 847 nm, 1.50663 for 1064 nm, 1.50059 for 1555 nm. For reference the commonly used fused silica index variation would be 1.47607, 1.46782, 1.46071, 1.45256, 1.44963 and 1.44396 respectively.

QUESTION 13) Dihedral angle offset(s) and the manufacturing tolerance.
ANSWER 13) The Dihedral angle offsets are zero with a manufacture tolerance such that the beam deviation is less than + or - 3 arc seconds. These were not confirmed by independent quality control process beyond industry practice at Edmund.

QUESTION 14) Radius of curvature of the front surfaces of cubes if applicable.
ANSWER 14) The radius of curvature of the aperture of the cubes is infinity. There is no intended power from the aperture on these retroreflecotrs.

QUESTION 15) Flatness of cubes surfaces (as a fraction of wavelenth);
ANSWER 15) The flatness of the cubes surfaces (as a function of 633 nm light) is such that after the three back faces and two aperture crossings the beam remains lambda / 8.

QUESTION 16) Whether or not the cubes are coated and with what material.
ANSWER 16) The aperture of the cubes are coated with the Edmund Custom V2 (532 and 1064) Anti reflection coating. The back faces have vacuum deposited silver.

Figure 2: The ANDERR MAA (a) and FCAL (b) spacecraft.

Flight Hardware Overview of the ANDERR (Questions 1,2,3)

There were a total of 5 components deployed as an Internal Cargo Unit (ICU) from the NASA STS-116 Discovery Flight shown in Figure 3. This deployment object will not be spinning about the long axis of the cylinder (ICU) and is separated from the Cargo Bay with delta-V in the range 0.45 to 0.61 meters per second. The ICU system of 5 components will separate approximately 40 seconds later into components Cylinder1, MAA, Disk1, FCAL, Cylinder2, under spring forces using a light band deployment systems as shown in Figure 3. Only the spherical objects MAA (Figure 4) and FCAL (Figure 5) have retro reflectors in a spherical configuration of these five objects. These were manufactured and assembled at NRL using a variety of custom and cots components. The surface finish on the MAA is aluminum with black anodized and gold irridited. The surface finish on the FCAL is white paint and nickel coated brass. Under a nominal deployment the MAA will be spinning a 5 revolutions per minute and the FCAL will be negligible, however the deployment resulted in a negligable spin to both spacecraft.. Confirmation using ground techniques will be desired days after deployment. There will be high definition video for the first few minutes for accurate comparison. The spin is required on the follow-on ANDE flight for the accurate sensing of the species constituents and the thermal control for the modulators and other hardware. The ILRS nomenclature for the MAA and FCAL will be ANDERRA (Active) and ANDERRP (Passive) for the CPF prediction names. While both have active RF transmitters sending measurements to the ground, this naming convention is consistent with the laser diode sources on the MAA. The MAA sphere has COSPAR 0605506, catalog 29664, and SIC 1071. The FCAL sphere has COSPAR 0605510, catalog 29667, and SIC 1072.

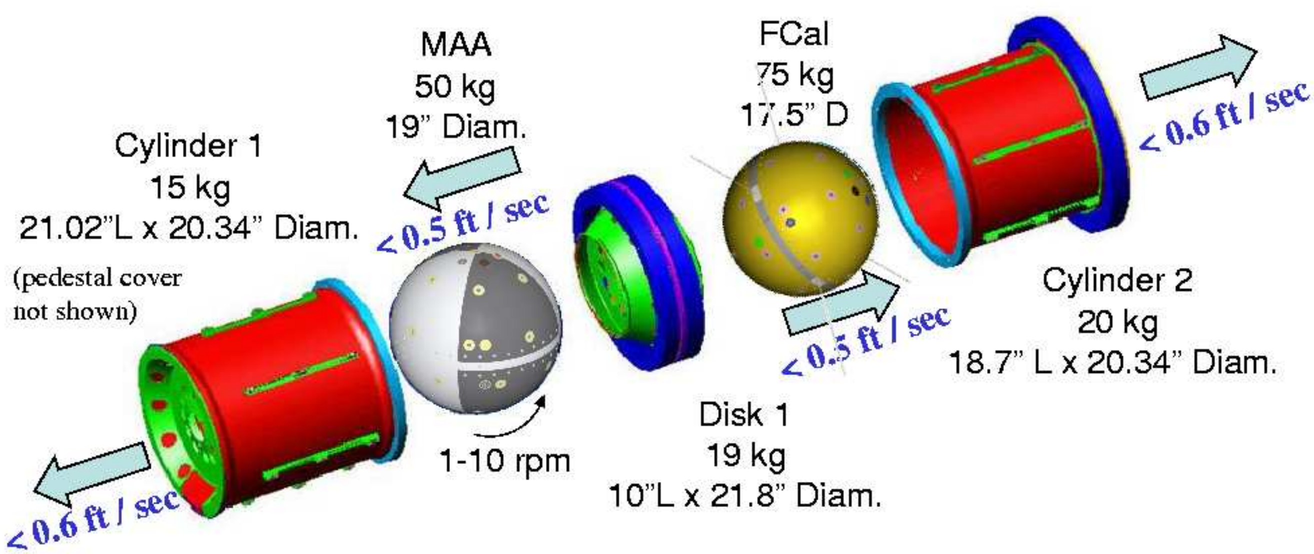

Figure 3: The ANDERR deployer from the Space Shuttle

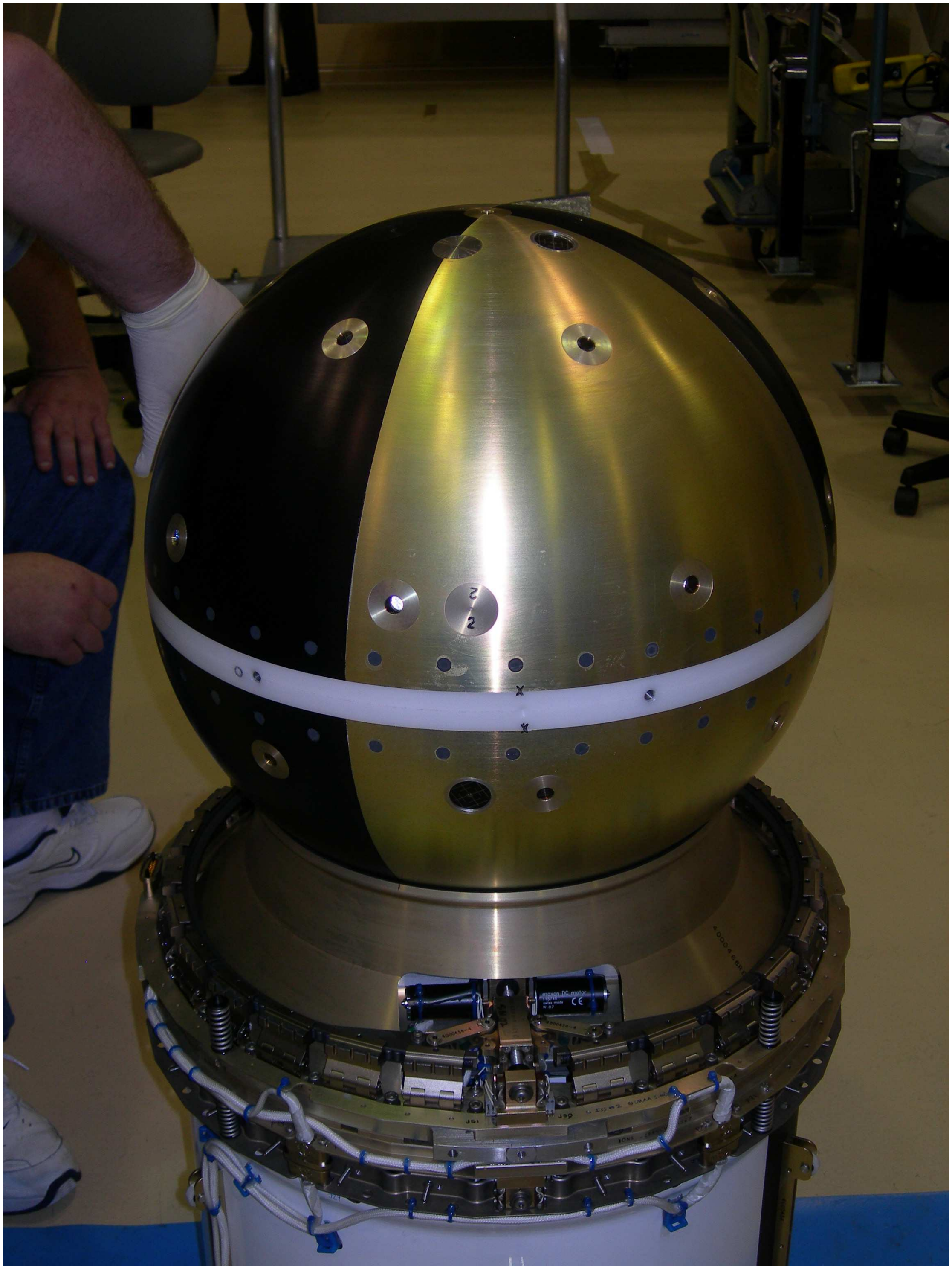

Figure 4: The ANDERR MAA spacecraft

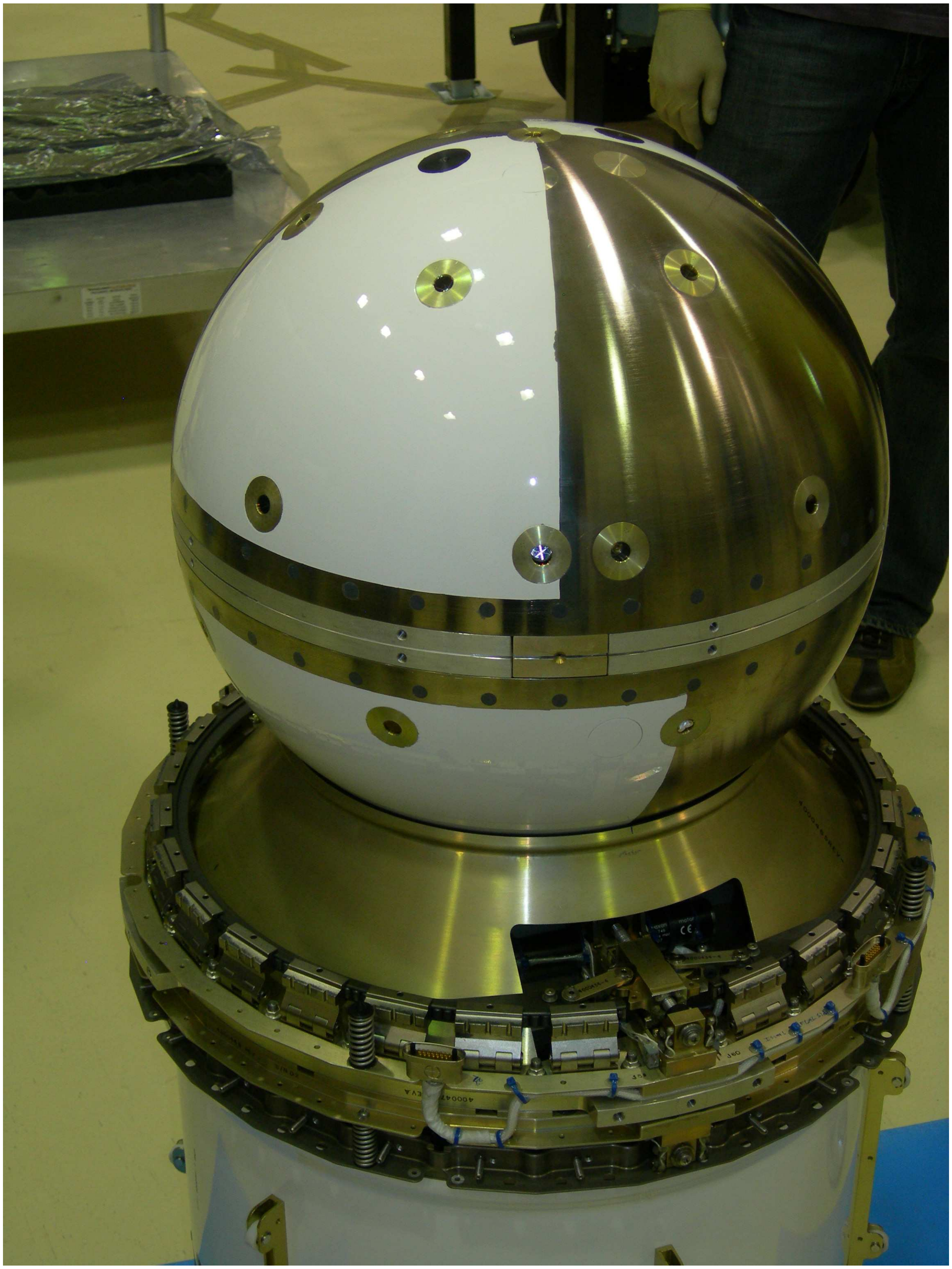

Figure 5: The ANDERR FCAL spacecraft

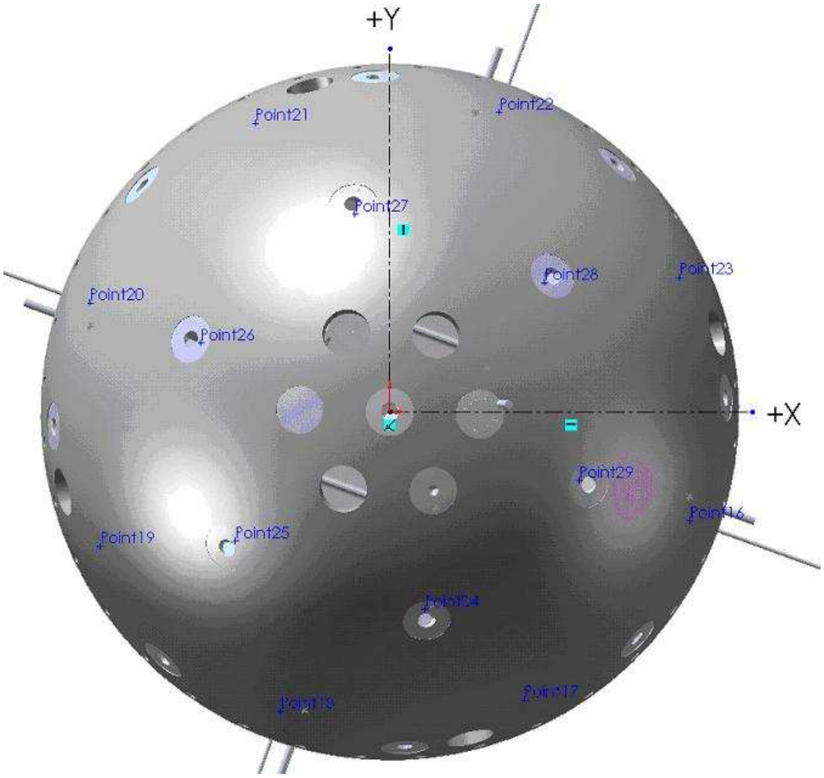

Figure 6: The FCal lower view

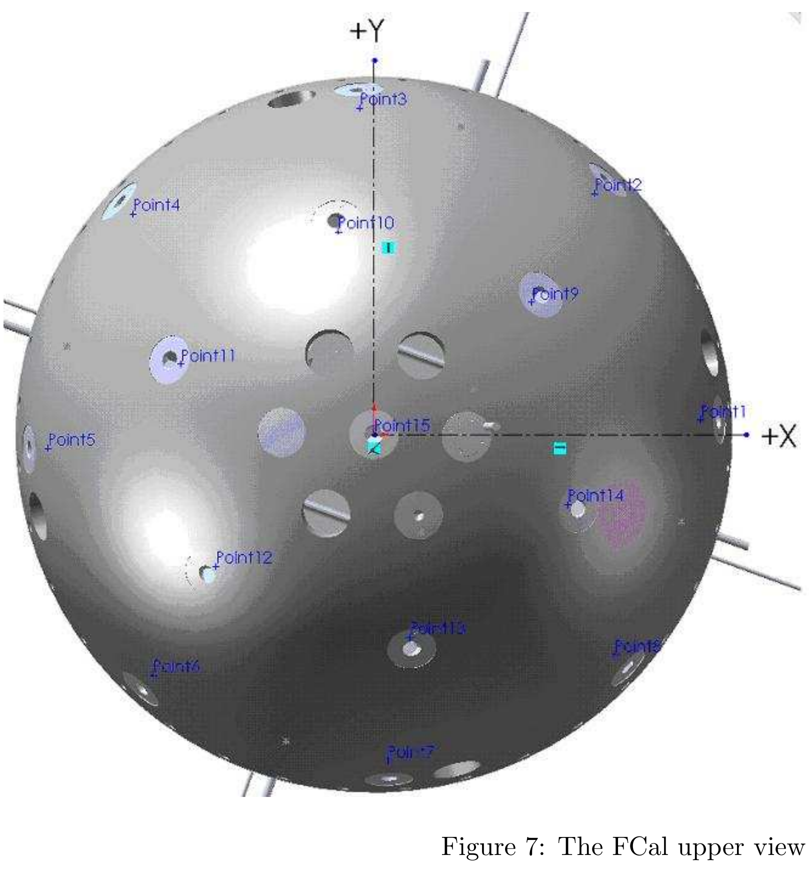

Figure 7: The FCal upper view

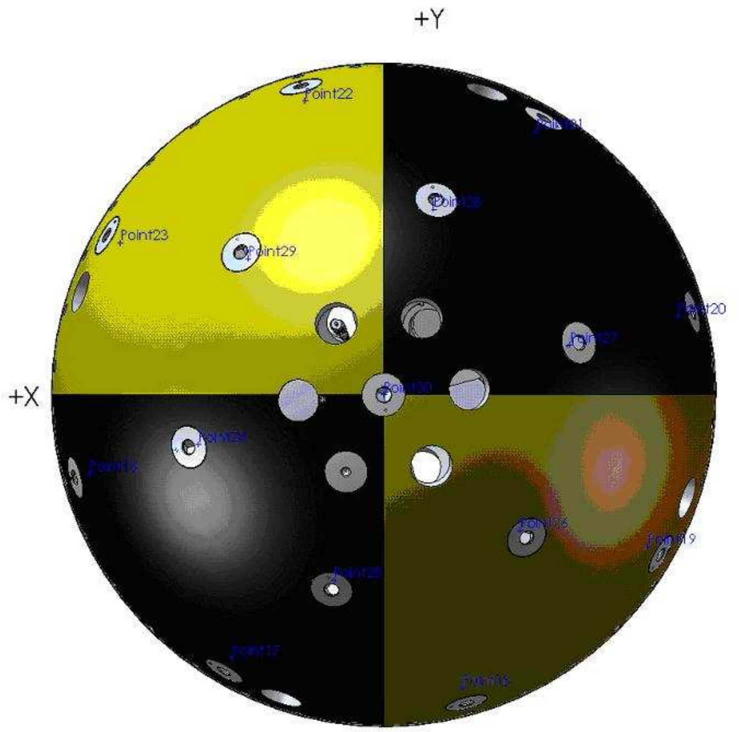

Figure 8: The MAA lower view

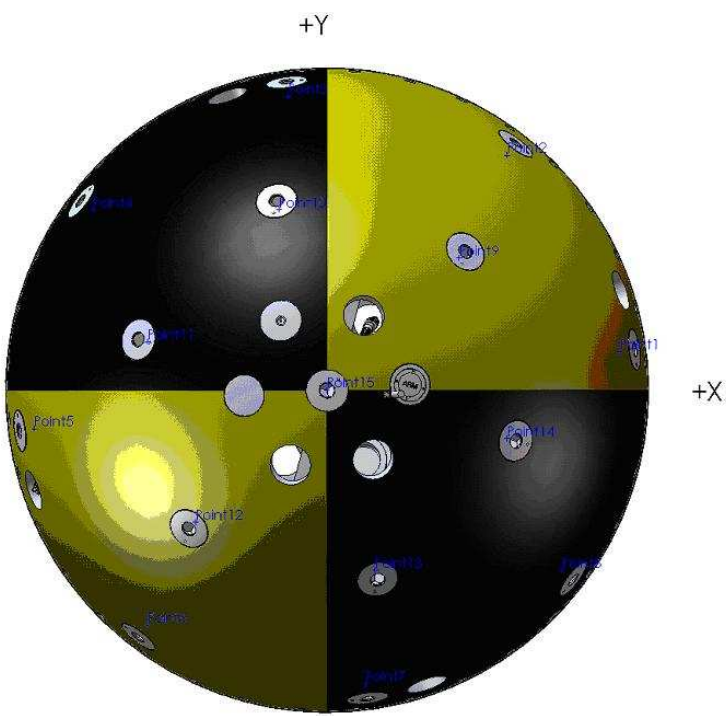

Figure 9: The MAA upper view

Retro Reflectors and corrections the ANDERR MAA (Active) and FCAL (Passive) (Questions 4 through 16)

There are thirty retro reflectors on each sphere in an orientation of + / - 90, 52.5 and 15 degrees from the equator, with one, six and eight retroreflectors per band respectively. The retro reflectors are Edmund Optics NT45-202 12.7 mm prism corner cubes as shown in Figure 11. These have aperture to vertex (height) distances for 10.16 mm as shown in Figure 10. The exposed aperture is 0.42 inches (10.67 mm) diameters as shown in Figure 13. After mounting in the universal holder shown in Figure 14, the optical testing did not include metric performance testing. These holders then threaded from the inside of the sphere. The aperture of each reflector is (0.058 inches) 1.52 mm below the holder lip as shown in Figure 12, which has negligible impact on the theoretical incidence angle functionality and cross section. Details of the mounting are shown in expanded view Figures 16 and 15. The retroreflector spatial design (number and orientation) is a reuse of that used on the Starshine flights and consists of 30 reflectors on a sphere providing overlap and cross section shown in Figure 17. Estimates of the 532nm optical cross section of this design exceed 0.05 Million square meters in the worst orientation with more typical values near 0.12. The use of the COTS retro reflectors has been used successfully by NRL on other very LEO missions and the tolerancing and non-rad-hard substrates are a research area but not expected to degrade over the short lifespan of these satellites.

The aperture coatings on each reflector is the 2V (532 and 1064 nm) COTS antireflective product from Edmunds. The back faces are vacuum deposited silver with inconel and black over paint. The orientation of each reflector is radially outward, with vertex of each reflector located at positions shown in Tables 1 and 2. The number of significant digits in the inches columns is directly from the 3-d modeling software. The metric and computed radius and dispersion are numerically derived from the inches measurements. The as-built hardware generally agrees with the design model to + / - 0.015 inches or + / - 0.38 mm. These have mean values of 229.41 (stdev 0.64) and 209.88 (stdev 0.23) mm for MAA and FCAL respectively. Given that the aperture to vertex distance is 10.16 and index of the BK7 material at 532 nm being 1.51947, the optical phase center will be 5.28 mm inside the sphere of vertex locations. The center of mass correction for the MAA (ACTIVE) is 224.1 mm and for FCAL (PASSIVE) is 204.6 mm. It should be noted that the center of mass of each object is slightly offset from the frame used for measuring the vertex locations by at most 1.1 millimeter and that spin rate and orientation would need to be modeled for any improvements. Some of this orientation data will be in the experimental data that is downlinked and available from the web link [10].

The aperture of each retroreflector has a small recession below the satellite surface as shown in Figure 12. This has been measured to be less than 1.55 mm at the center of the aperture. Due to the curvature over the size of the aperture this is 0.061 in the center and 0.058 inches. This was chosen to minimize the overall surface deviations and retain the average curvature of the outer sphere diameter.

Most of the design was done using English units with mechanical tolerancing being + / - 15 mils. The metric equivalent (0.38 mm) have been included for the reader and were in most all cases derived.

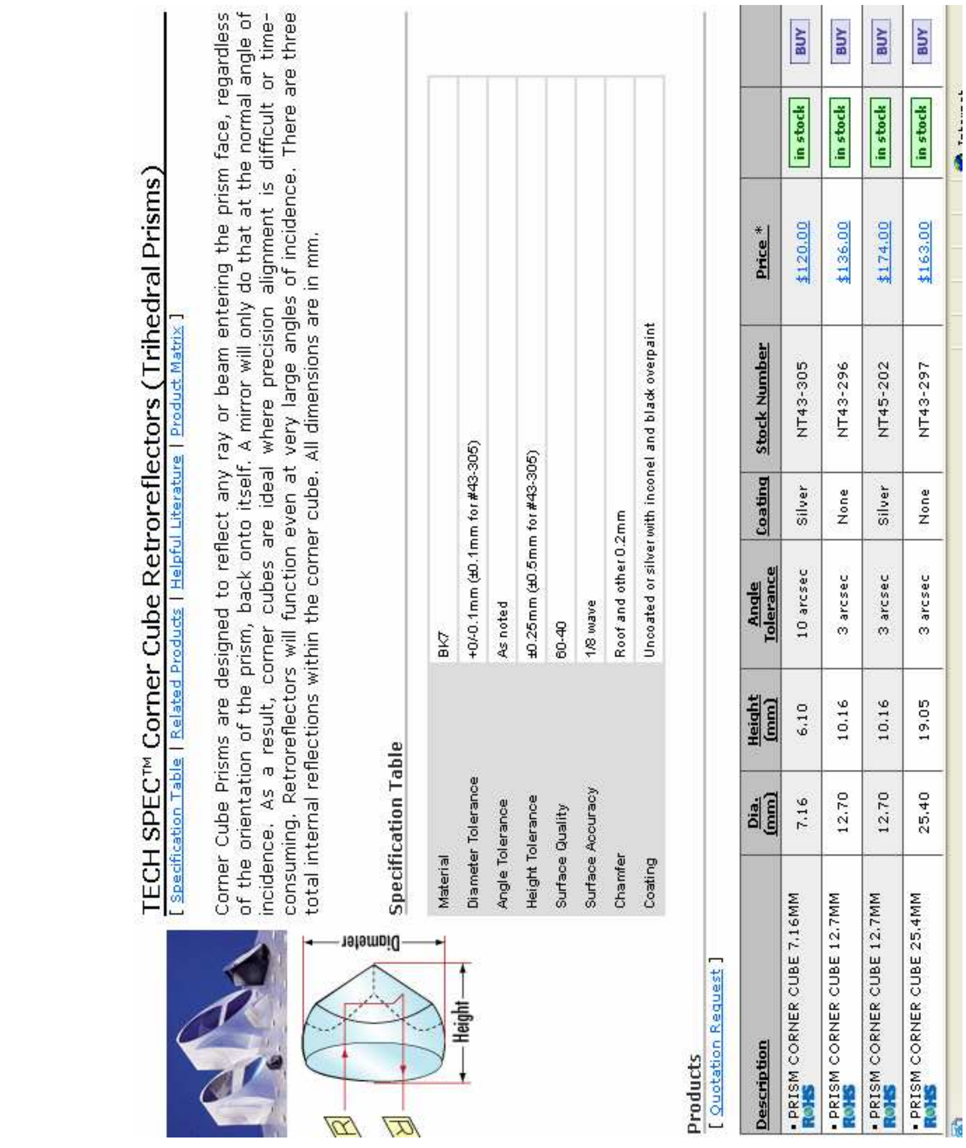

TECH SPEC™ Corner Cube Retroreflectors (Trihedral Prisms)

[Specification Table | Related Products | Helpful Literature | Product Matrix]

Corner Cube Prisms are designed to reflect any ray or beam entering the prism face, regardless of the orientation of the prism, back onto itself. A mirror will only do that at the normal angle of incidence. As a result, corner cubes are ideal where precision alignment is difficult or time-consuming. Retroreflectors will function even at very large angles of incidence. There are three total internal reflections within the corner cube. All dimensions are in mm.

Specification Table

Material	BK7
Diameter Tolerance	+0/-0.1mm (±0.1mm for #43-305)
Angle Tolerance	As noted
Height Tolerance	±0.25mm (±0.5mm for #43-305)
Surface Quality	60-40
Surface Accuracy	1/8 wave
Chamfer	Roof and other 0.2mm
Coating	Uncoated or silver with inconel and black overpaint

Products

[Quotation Request]

Description	Dia. (mm)	Height (mm)	Angle Tolerance	Coating	Stock Number	Price *		
• PRISM CORNER CUBE 7.16MM RoHS	7.16	6.10	10 arcsec	Silver	NT43-305	$120.00	in stock	BUY
• PRISM CORNER CUBE 12.7MM RoHS	12.70	10.16	3 arcsec	None	NT43-296	$136.00	in stock	BUY
• PRISM CORNER CUBE 12.7MM RoHS	12.70	10.16	3 arcsec	Silver	NT45-202	$174.00	in stock	BUY
• PRISM CORNER CUBE 25.4MM RoHS	25.40	19.05	3 arcsec	None	NT43-297	$163.00	in stock	BUY

Figure 10: The retro reflectors vendor basic components

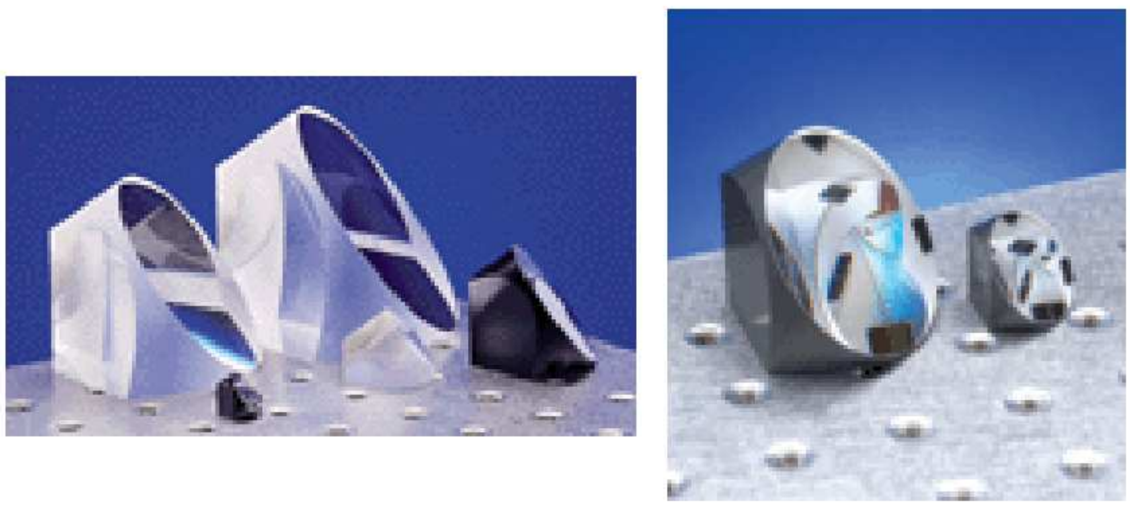

Figure 11: The type of retroreflectors

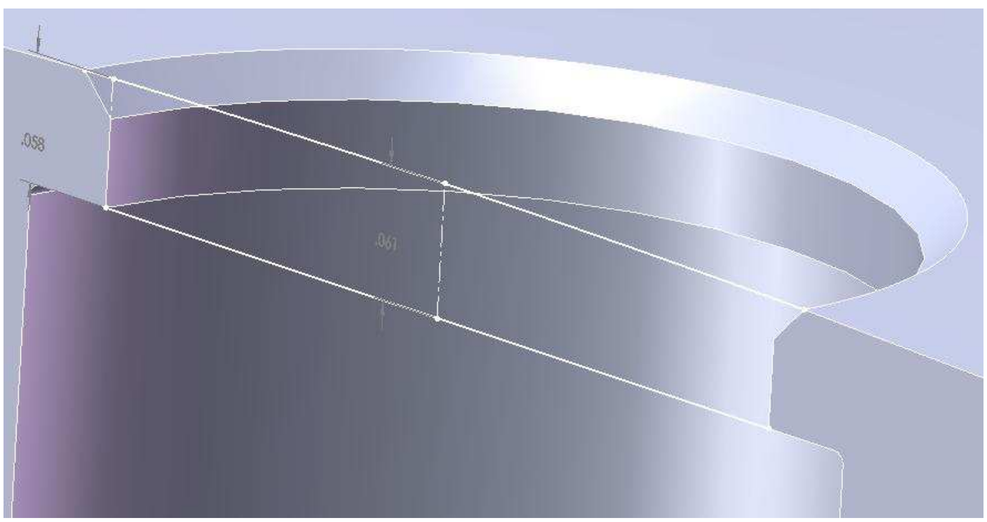

Figure 12: The retroreflector aperture is recessed below the surface (0.058 inches)

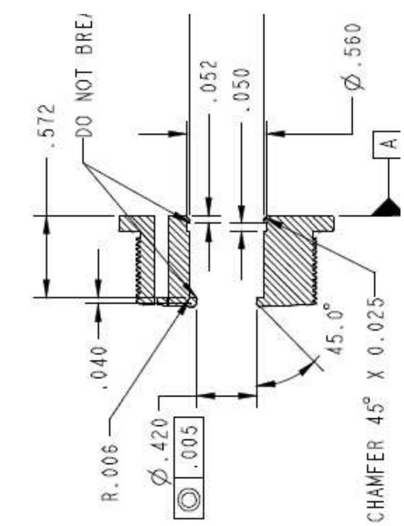

Figure 13: The retro reflector detail mounting with diameter of exposure

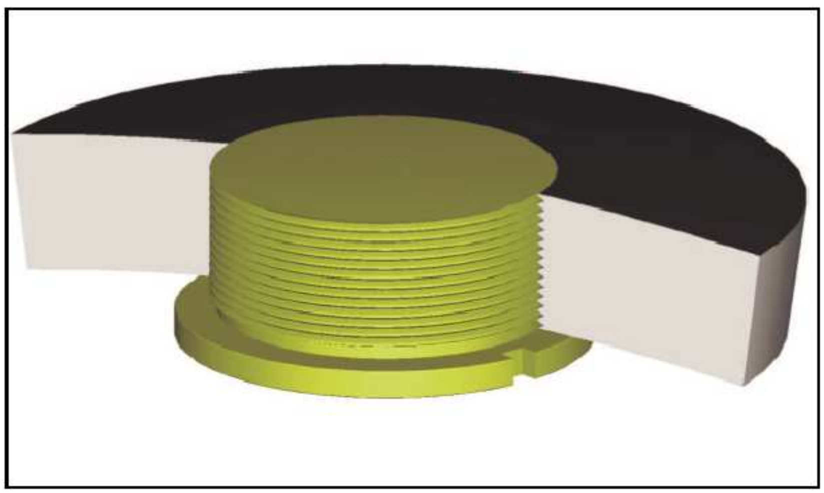

Figure 14: The retro holder and sphere surface

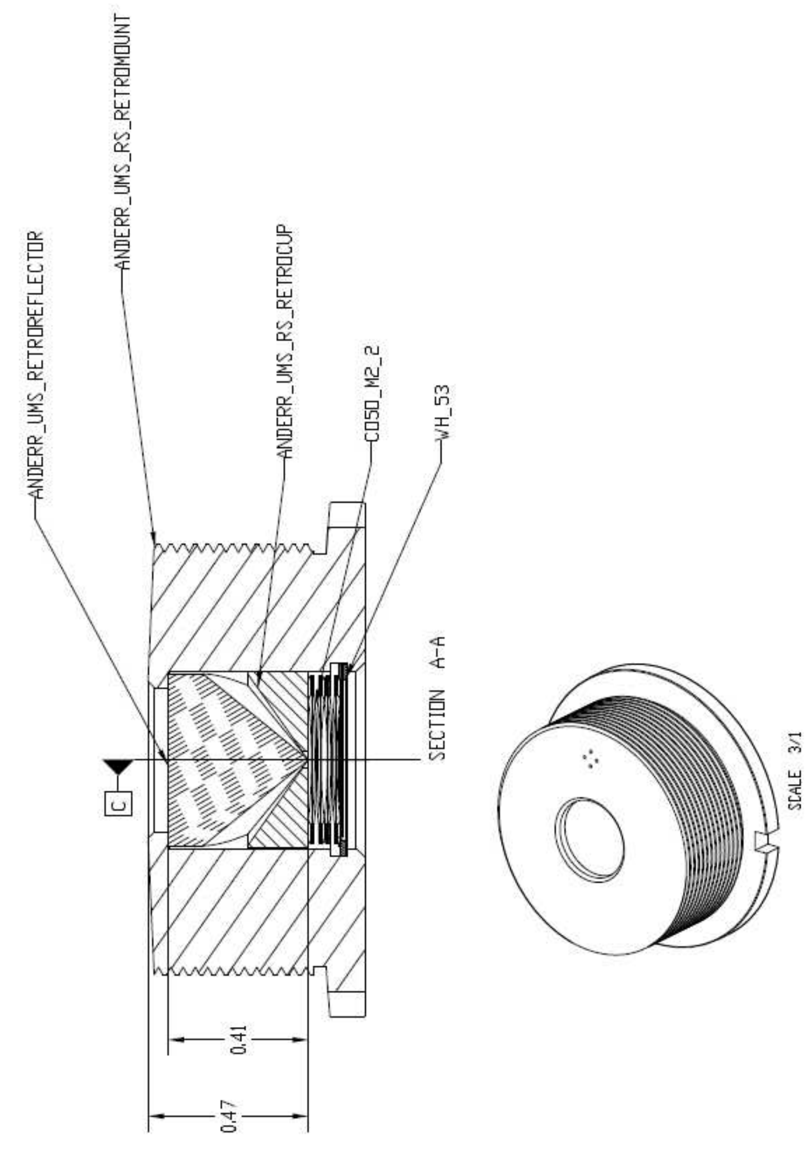

Figure 15: The retro holder and sphere surface

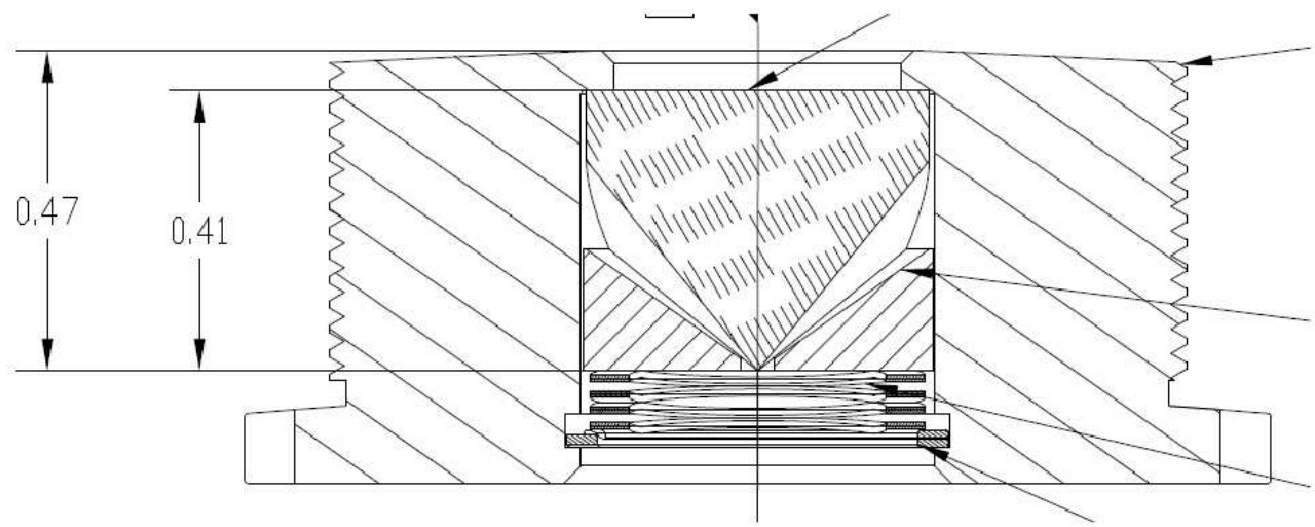

Figure 16: The retro reflector detail and mounting view

Reflector	x-inches	y-inches	z-inches	x-mm	y-mm	z-mm	mag	deviation
1	+7.9662	+0.3478	+2.1364	+202.34	+8.83	+54.26	209.68	-0.20
2	+5.3856	+5.8774	+2.1364	+136.79	+149.29	+54.26	209.63	-0.25
3	-0.3478	+7.9667	+2.1364	-8.83	+202.35	+54.26	209.69	-0.19
4	-5.8785	+5.3867	+2.1364	-149.31	+136.82	+54.26	209.67	-0.21
5	-7.9656	-0.3478	+2.1364	-202.33	-8.83	+54.26	209.66	-0.22
6	-5.3854	-5.8771	+2.1364	-136.79	-149.28	+54.26	209.62	-0.26
7	+0.3479	-7.9677	+2.1364	+8.84	-202.38	+54.26	209.71	-0.16
8	+5.8798	-5.3879	+2.1364	+149.35	-136.85	+54.26	209.71	-0.17
9	+3.8494	+3.2300	+6.5500	+97.77	+82.04	+166.37	209.69	-0.19
10	-0.8725	+4.9485	+6.5500	-22.16	+125.69	+166.37	209.69	-0.19
11	-4.7217	+1.7186	+6.5500	-119.93	+43.65	+166.37	209.69	-0.19
12	-3.8514	-3.2317	+6.5500	-97.83	-82.09	+166.37	209.73	-0.15
13	+0.8734	-4.9531	+6.5500	+22.18	-125.81	+166.37	209.76	-0.12
14	+4.7229	-1.7190	+6.5500	+119.96	-43.66	+166.37	209.71	-0.17
15	+0.0000	0.0000	+8.2601	0.00	0.00	+209.81	209.81	-0.07
16	+7.5114	-2.7339	-2.1364	+190.79	-69.44	-54.26	210.16	+0.28
17	+3.3761	-7.2400	-2.1364	+85.75	-183.90	-54.26	210.04	+0.16
18	-2.7358	-7.5164	-2.1364	-69.49	-190.92	-54.26	210.29	+0.41
19	-7.2493	-3.3801	-2.1364	-184.13	-85.85	-54.26	210.29	+0.41
20	-7.5119	+2.7341	-2.1364	-190.80	+69.45	-54.26	210.17	+0.29
21	-3.3769	+7.2418	-2.1364	-85.77	+183.94	-54.26	210.09	+0.21
22	+2.7375	+7.5211	-2.1364	+69.53	+191.04	-54.26	210.41	+0.54
23	+7.2490	+3.3803	-2.1364	+184.12	+85.86	-54.26	210.28	+0.40
24	+0.8744	-4.9588	-6.5500	+22.21	-125.95	-166.37	209.85	-0.03
25	-3.8615	-3.2402	-6.5500	-98.08	-82.30	-166.37	209.93	+0.06
26	-4.7382	+1.7246	-6.5500	-120.35	+43.80	-166.37	209.96	+0.08
27	-0.8742	+4.9581	-6.5500	-22.20	+125.94	-166.37	209.84	-0.04
28	+3.8615	+3.2402	-6.5500	+98.08	+82.30	-166.37	209.93	+0.06
29	+4.7333	-1.7228	-6.5500	+120.23	-43.76	-166.37	209.88	-0.00
30	0.0000	0.0000	-8.2601	0.00	0.00	-209.81	209.81	-0.07
cm	0.0000	0.0000	0.0250	0.00	0.00	0.64	0.64	

Table 1: Retroreflector vertex locations for the MAA.

Reflector	x-inches	y-inches	z-inches	x-mm	y-mm	z-mm	mag	deviation
1	+8.6577	+1.1741	+2.3484	+219.91	+29.82	+59.65	229.80	+0.39
2	+5.3187	+6.9573	+2.3484	+135.09	+176.72	+59.65	230.30	+0.89
3	-1.1316	+8.6857	+2.3484	-28.74	+220.62	+59.65	230.34	+0.93
4	-6.9148	+5.3467	+2.3484	-175.64	+135.81	+59.65	229.89	+0.48
5	-8.6432	-1.1036	+2.3484	-219.54	-28.03	+59.65	229.22	-0.19
6	-5.3042	-6.8868	+2.3484	-134.73	-174.92	+59.65	228.71	-0.70
7	+1.1461	-8.6152	+2.3484	+29.11	-218.83	+59.65	228.67	-0.73
8	+6.9293	-5.2762	+2.3484	+176.00	-134.02	+59.65	229.12	-0.29
9	+3.8956	+3.9236	+7.1768	+98.95	+99.66	+182.29	230.11	+0.71
10	-1.4169	+5.3501	+7.1768	-35.99	+135.89	+182.29	230.20	+0.79
11	-5.3054	+1.4588	+7.1768	-134.76	+37.05	+182.29	229.70	+0.29
12	-3.8808	-3.8528	+7.1768	-98.57	-97.86	+182.29	229.18	-0.23
13	+1.4306	-5.2768	+7.1768	+36.34	-134.03	+182.29	229.16	-0.25
14	+5.3191	-1.3881	+7.1768	+135.11	-35.26	+182.29	229.62	+0.22
15	0.0000	0.0000	+9.0434	0.00	0.00	+229.70	229.70	+0.30
16	+8.4128	-2.2170	-2.3484	+213.69	-56.31	-59.65	228.89	-0.52
17	+4.3551	-7.4954	-2.3484	+110.62	-190.38	-59.65	228.12	-1.28
18	-2.2440	-8.3665	-2.3484	-57.00	-212.51	-59.65	227.96	-1.44
19	-7.5234	-4.3126	-2.3484	-191.09	-109.54	-59.65	228.20	-1.21
20	-8.3992	+2.2878	-2.3484	-213.34	+58.11	-59.65	229.02	-0.39
21	-4.3406	+7.5659	-2.3484	-110.25	+192.17	-59.65	229.44	+0.04
22	+2.2595	+8.4408	-2.3484	+57.39	+214.40	-59.65	229.82	+0.42
23	+7.5379	+4.3831	-2.3484	+191.46	+111.33	-59.65	229.37	-0.04
24	+5.3209	-1.3885	-7.1768	+135.15	-35.27	-182.29	229.65	+0.25
25	+1.4305	-5.2762	-7.1768	+36.33	-134.02	-182.29	229.15	-0.25
26	-3.8810	-3.8530	-7.1768	-98.58	-97.87	-182.29	229.18	-0.22
27	-5.3042	+1.4585	-7.1768	-134.73	+37.05	-182.29	229.68	+0.28
28	-1.4160	+5.3467	-7.1768	-35.97	+135.81	-182.29	230.15	+0.74
29	+3.8955	+3.9235	-7.1768	+98.95	+99.66	-182.29	230.11	+0.71
30	0.0000	0.0000	-9.0434	0.00	0.00	-229.70	229.70	+0.30
cm	-0.0250	-0.0250	0.0250	-0.64	-0.64	0.64	1.10	

Table 2: Retroreflector vertex locations for the FCAL.

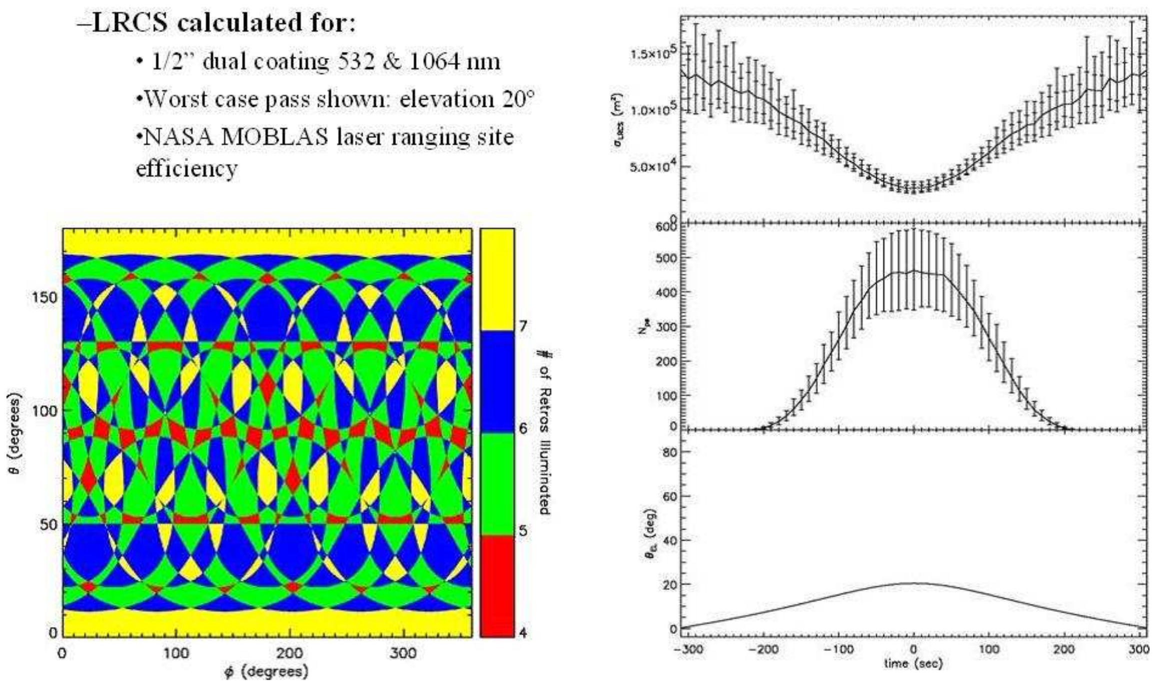

Figure 17: The LRCS and number of contributing reflectors and estimated link budget

Solar Reflection Details

The paint scheme of 8 quadrants of two varieties permits the measurement of solar flux variability. The plots in Figure 20 and 21 show the expected reflectance ratios for observing with the non-ranging bands on some of the SLR observatories. Details of these measurements were made and described in Abercrombie [4].

Radio and Optical Transmissions and Thermal Details

The US Naval Academy has designed and built the 2 Watt ERP downlink system for the MAA spacecraft which will transmit payload data at 145.825 MHz at nominally 2 minute intervals. This signal will have 20 MHz bandwidth. Much of the detail is described on the web site [9] and [8].

There are experiments planned for MAA which require known optical flux and as such there are laser diodes which will emit thru the universal mounting ports adjacent to the retro reflectors. These are operated nominally over Hawaii and will degrade the battery life (and hence the RF transmissions of payload data) late in the mission if used often over other areas. There are 6 output ports for the 810 nm laser firing at different rates each at 100 msec duration as shown in Figure 18. This system is actived by RF uplink and will function for 300 seconds. Proposals and details for activation on other geographic are being considered for research purposes.

The FCal transmitter operates at 436.81 MHz. The transmitter is an FM transmitter consisting of an exiter and power amplifier. The exciter is crystal controlled adn has a modulation input port for an audio signal or AFSK signal. The output level of the exciter is 10 mW. The exciter output is connected to the amplifier circuit. The amplifier is a singal IC device capable of a maximum of 800 milliwatts output. The output level is adjustable and has been set to 250 milliwats. The output of the amplifier is single ended with a low pass filter. It is routed to splitters with a 180 degree phase shift between the two outputs. The outputs are routed vias coaxial cable to two antenna boards on opposite sides of the FCAL.

The web site [10] has the most current realtime telemetry packets decoded. There are numerious plots available for the sensors at the web links [7]. Additionally the site [11] has details on the decomming of observations.

Mass Properties

The outer shell diameter for the MAA and FCAL are 19 inches and 17.5 inches respectively. The mass of the MAA is 114.73 lpb or 52.04 kg. The mass of the FCAL is 138.23 lbs or 62.70 kg. The MAA CG in the satellite xyz frame is at (0.025, 0.025, 0.025) inches. This is (-0.025, -0.025, 0.025) from the geometric center. The FCAL CG is at (0.000, 0.000, 0.025) inches.

The diagonal elements (off axis terms are zero) of the MAA Mass moment of Inertia are 14146.72, 14146.74, 14340.11 inlbm-in$\hat{2}$. The equivlanent for the FCAL are 15598.61, 15598.61, 15968.71 lbm-in$\hat{2}$.

Acknowledgment

The success of the results depend upon the observations and products of all the ILRS stations and coordinators. The support of all the contributions is gratefully acknowledged.

References

[1] Andrew C. Nicholas, et. al, "The Atmospheric Neutral Density Experiment (ANDE)", Proceedings of the 2002 AMOS Technical Conference, Maui HI, Sept 2002.

[2] Andrew C. Nicholas, S. Tonnard, I Galysh, P. Kalmanson, B. Bruninga, S. Ritterhouse, J. Englehardt, K. Doherty, J. McGuire, D. Niemi, H. Heidt, M. Hallada, "ANDE Risk Reduction Flight Observing Opportunities and Mission Update", Proceedings of the 2005 AMOS Technical Conference, Maui, HI, Sept 2005.

Laser diode output is 500 mW, in 100 msec pulses, at 810 nm

Pulse repetition varies between 1.5 and 4.25 Hz

Beam from each of 6 diodes is transmitted through 45 cm, 50 micron core fiber to 6 output apertures, formed by cleaved fibers

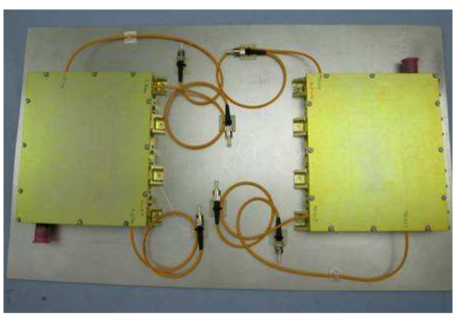

Board B	Board A
1.51 Hz	1.75 Hz
2.26 Hz	2.75 Hz
4.27 Hz	3.77 Hz

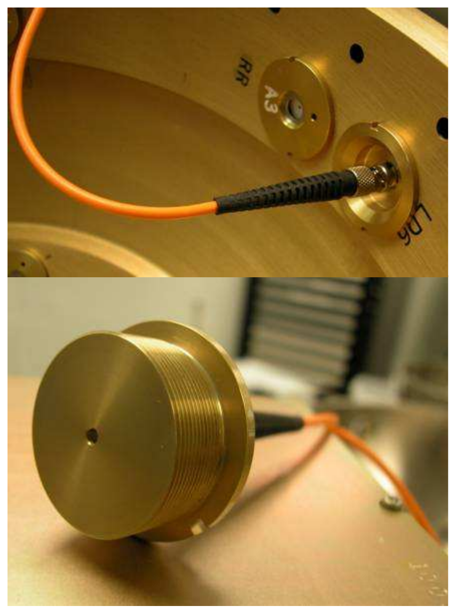

Figure 18: The ACTIVE sphere laser diodes and parameters

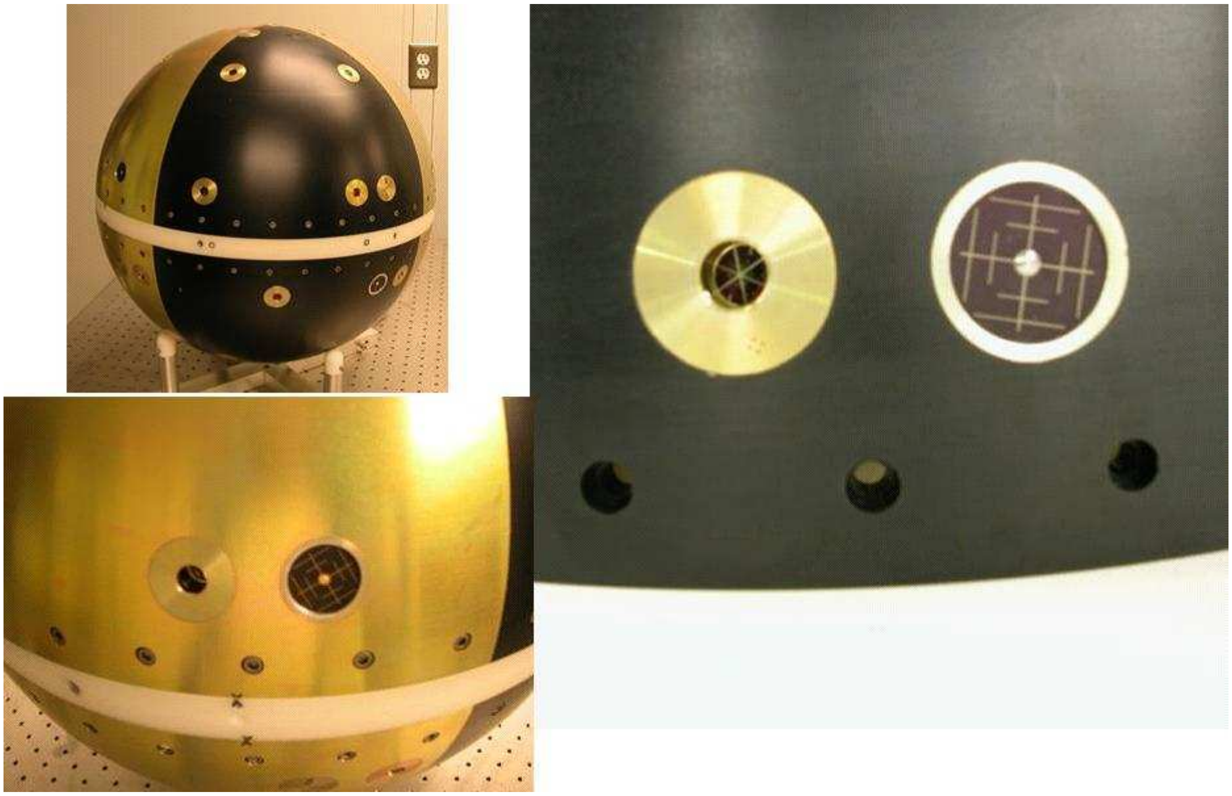

Figure 19: The ACTVIE sphere (MAA) details with both retroreflectors and laser output ports

[3] Andy Nicholas, "Atmospheric Neutral Density Experiment (ANDE) Risk Reduction Mission", Poster at the ILRS 15th Workshop, Canberra Australia, Oct 2006.

[4] Kira Abercromby, "Comparisons of Ground Truth and Remote Spectral Measurements of the FORMOSAT and ANDE Spacecraft", Proceedings of the 2006 AMOS Technical Conference, Maui HI, Sept 2006, pages 728 to 737.

[5] Robert Kessel, William Braun, Mark Davis, Amey Peltzer, Anne Reed, Ilene Sokolsky, John Vasquez, Paul Wright, "Development and on-orbit performance of moderate-cost spherical retroreflector arrays for the Starshine program", 13th ILRS workshop Proceedings, Washington D.C.

[6] Andrew Nicholas, G. C. Gilbreath, S. Thonnard, R. Kessel, R. Lucke, and C. P. Sillman, "The Atmospheric Neutral Density Experiment (ANDE) and Modulating Retroreflector In Space (MODRAS): Combined Flight Experiments for the Space Test Program", Proceedings of the SPIE Remote Sensing Conference, Agia Peligia, Crete, Greece, September 23-27 2002, Volume 4884, p49-58.

[7] http://web.usna.navy.mil/~bruninga/ande-raft-ops.html

[8] http://web.usna.navy.mil/~bruninga/fcal.html

[9] http://web.usna.navy.mil/~bruninga/ande.html

[10] http://www.g4dpz.me.uk/ANDE/home.do

[11] http://www.ne.jp/asahi/hamradio/je9pel/anderaft.html

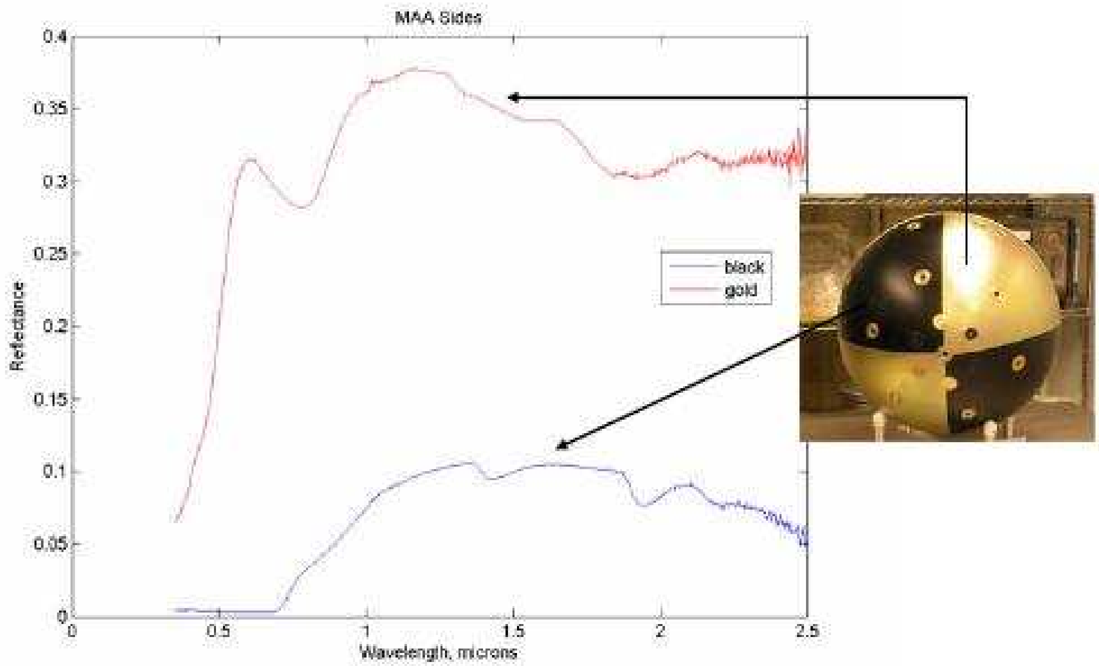

Fig. 7. The reflectance spectra for the sides of the MAA sphere. The blue line represents the black anodized aluminum while the red line represents the gold surface coating (irridite) finish.

Figure 20: The spectral response of the MAA from Reference [4]

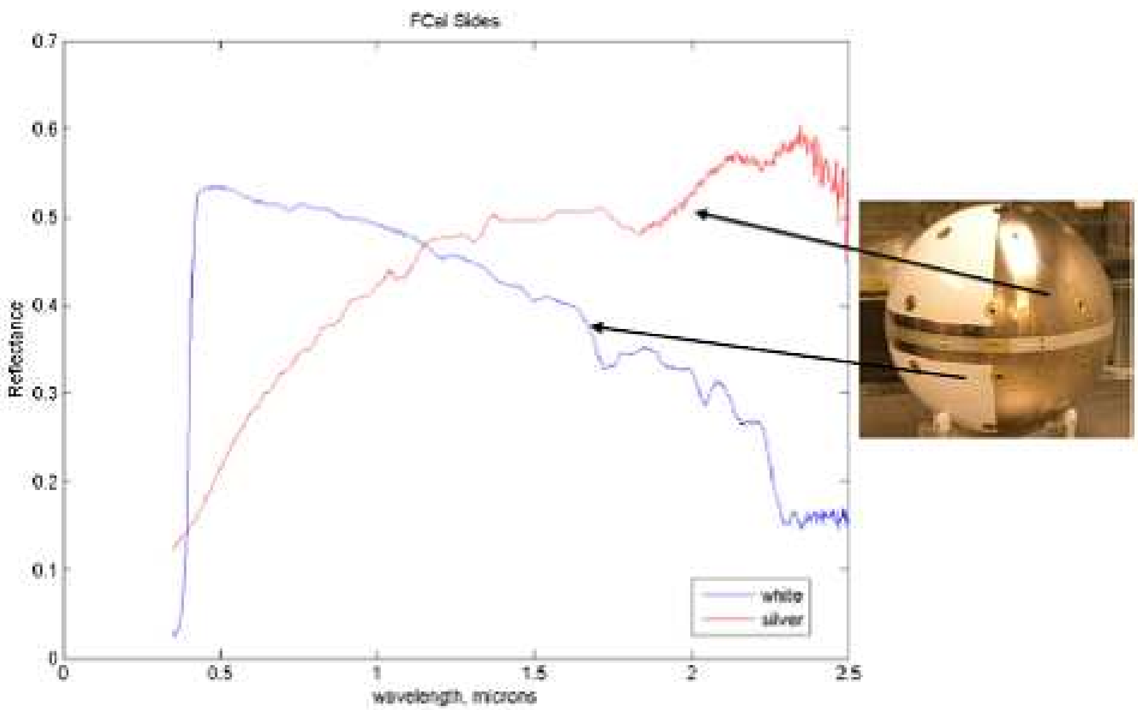

Figure 21: The spectral response of the FCAL from Reference [4]